A REPORT ON

"DC-Link Voltage Control Technique for Single-phase Two-stage Photovoltaic Grid-connected System"

(INFORMATIVE REPORT)

2016-17

SUBMITTED BY:

STUDENTS OF FINAL YEAR **ELECTRICAL**

UNDER THE GUIDANCE OF

Prof. ANKUR UPADHYAY

Anjuman-I-Islam's
KALSEKAR TECHNICAL CAMPUS
School of Engineering and
Technology New Panvel

A REPORT ON

"DC-Link Voltage Control Technique for Single-phase Two-stage Photovoltaic Grid-connected System"

(INFORMATIVE REPORT)

2016-17

New Panvel

Submitted to:

Prof. ANKUR UPADHYAY

Submitted By:

NAME	**ROLLNO.**
AMARKANT SHARMA	13EE54
SHAIKH ABDUL KHALID	13EE46
SHAIKH MOHD USMANGANI	13EE49
KHOJA FAIYAZ PYAREALI	13EE31

Prof. A.UPADHYAY	Prof. S. KALEEM	Dr. A. R. HONNUTAGI
(GUIDE)	(H.O.D)	(DIRECTOR)

ACKNOWLEDGEMENT

We would like to acknowledge the contributions of those who assisted in the preparation of this report.

We are particularly grateful for the work done by members of my group. Before we get into this report we would like to thanks to the members of the group who are apart of this report and have given their unending contribution from start to end of this report.

We would like to thank our **Prof. ANKUR UPADHYAY** for providing as the required guidance in process of preparing the report. We would also like to express our deep regards and gratitude to the director **Dr. ABDUL RAZZAK HONNUTAGI**.

We would like to express our gratitude towards our parents for their kind co-operation and encouragement which help us in completion of this project..

We have taken lots of efforts in this project. However, it would not have been possible without the kind support and help of many individuals and organizations. We would like to extend our sincere thanks to all of them.

PREFACE

We take the opportunity to present this report "**DC-Link Voltage Control Technique for Single-phase Two-stage Photovoltaic Grid-connected System".** The object of this report is to make a control technique with low cost.

The report is supported by images to bring out the purpose and message. We have made sincere attempts and taken every care to present this report in precise and compact form, the language being as simple as possible.

The task of completion of the project though being difficulty was made quite simple , interesting and successful due to deep involvement and complete dedication of our group members.

CERTIFICATE

This is to certify that the report entitled "**DC-Link Voltage Control Technique for Single-phase Two-stage Photovoltaic Grid-connected System**" submitted by **SHARMA AMARKANT, SHAIKH MOHD USMANGANI , SHAIKH ABDUL KHALID , KHOJA FAIYAZ PYAREALI** in partial fulfillment of the requirement for the award of Bachelor of engineering in "**ELECTRICAL ENGINEERING**"is an authentic word carried by the under my supervision and guidance.

Date:

Examiner _____

Prof. Ankur Upadhyay _____

(Guide)

Prof. S. Kaleem _____

(HOD)

Dr. Abdul Razzak Honnutagi

(Director)

ABSTRACT

Control techniques, applied to single-phase two stage grid-connected photovoltaic (PV) systems, mainly achieve functions of maximum power point tracking (MPPT), voltage adjustment at inverter DC-link, and grid current control. Conventional control techniques require measurements of PV voltage and current, DC-link voltage, and grid voltage and current. In this paper, conventional technique is proposed which keeps PV sensors, but eliminates the expensive high DC link voltage sensor by mitigating the inverter DC-link voltage control loop. Alternatively, voltage regulation at inverter DC link is achieved through power balance guarantee at this link. Hence, control complexity is minimized and system stability is enhanced. Moreover, the entire system implementation is simplified and its dynamic response is improved during sudden irradiance changes. Simulation work is carried out to verify the effectiveness of conventional one regarding their transient and steady-state performance under varying irradiance conditions.

.

DECLARATION

I declare that this written submission represents my ideas in my own words and where others ideas or words have been included, I have adequately cited and referenced the original sources. I also declare that I have adhered to all principle so academic honesty and integrity and have not misrepresented or fabricated or falsified any idea/data/fact/source in my submission. I understand that any violation of the above will be cause for disciplinary action by the Institute and can also evoke penal action from the sources which have thus not been properly cited or from whom proper permission has not been taken when needed.

DATE ……..

PLACE……

(NAME OF THE STUDENT)

SHARMA AMARKANT ……..

SHAIKH MOHD USMANGANI ……..

SHAIKH ABDUL KHALID ……..

KHOJA FAIYAZ PYAREALI …….

Table of content

LIST OF FIGURES

CHAPTER 1

INTRODUCTION

Nowadays, common distributed energy resources (DERs), particularly PV sources, are increasingly being connected to utility for best utilization of their produced electric power. For PV-grid interface, a number of methods are used, among which the string inverter technology is widely used at present. Among current renewable energy resources, photovoltaic (PV) energy has gained much interest as a noise and pollution free source. Furthermore, it has the ability to be expanded and utilized in arid area. In this method, a number of PV modules are connected in a series arrangement; called a string, and each string has its own inverter. Thus, the MPP of each PV string is separately optimized and the PV system can be expanded easily by adding additional strings with their relative inverters.

One of the major concerns in the power sector is the day-to-day increasing power demand but the unavailability of enough resources to meet the power demand using the conventional energy sources. Demand has increased for renewable sources of energy to be utilized along with conventional systems to meet the energy demand. Renewable sources like wind energy and solar energy are the prime energy sources which are being utilized in this regard. The continuous use of fossil fuels has caused the fossil fuel deposit to be reduced and has drastically affected the environment depleting the biosphere and cumulatively adding to global warming. Solar energy is abundantly available that has made it possible to harvest it and utilize it properly. Solar energy can be a standalone generating unit or can be a grid connected generating unit depending on the availability of a grid nearby. Thus it can be used to power rural areas where the availability of grids is very low. Another advantage of using solar energy is the portable operation whenever wherever necessary.

For low-power (< 10 kW) applications, DERs are usually connected to the AC grid through a single-phase voltage source inverter (VSI) at low voltage (110-220V) . For successful PV string-grid interface, a number of requirements arise ; maximum power point tracking (MPPT), voltage regulation at inverter DC-link, and grid current control. To achieve the latter, two topologies exist ; single-stage and two-stage topologies. The single-stage topology involves a single inverter stage to achieve all the previous tasks in order to reduce component count and

increase conversion efficiency. However, this inverter must be carefully designed to handle the double line frequency voltage ripples that appear at its DC-link due to single-phase connection . Furthermore, large electrolytic capacitors must be connected to the PV string to limit these ripples propagation in the PV power, thus reducing inverter life-time . Alternatively, two-stage topology is investigated in which a power decoupling DC-DC stage is added before the inverter stage. This stage decouples the energy change between the PV string and the inverter DC-link which limits the voltage ripple impact on the PV source. Moreover, transformation of PV voltage level can be achieved using this additional stage thus expanding its operating range .

Conventionally, maximum power point tracking (MPPT) is achieved by the DC/DC converter stage while the second inverter stage inhibits two control loops to deliver power to the grid . The first is an outer voltage control loop at the inverter DC-link and the second is an inner current control loop which forces the inverter to produce a sinusoidal grid current at low THD and almost unity power factor. Thus, the conventional control strategy for single-phase two-stage system requires measurement of PV voltage and current to detect PV power and achieve MPPT, DC-link voltage, and grid voltage and current.

CHAPTER 2

SYSTEM UNDER CONSIDERATION

The considered system is a 1.5 kW, 220 V, 50 Hz single-phase transformer-less two-stage grid–connected PV system as shown in Fig. 1. The PV source is a string consisting of ten KD135SX_UPU PV arrays connected in series. The first stage is a boost converter responsible for MPPT, PV voltage boosting, and decoupling between PV source and the DC-link. The second stage inhibits a current-controlled voltage source inverter (VSI) for grid interface.

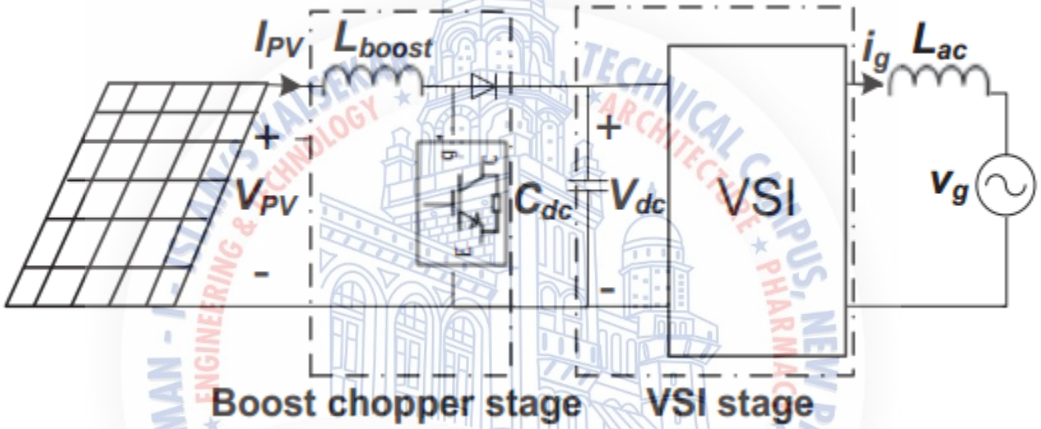

Fig 1. PV-grid connected system under consideration

2.1. Boost Converter

Boost converter steps up the input voltage magnitude to a required output voltage magnitude without the use of a transformer. The main components of a boost converter are an inductor, a diode and a high frequency switch. These in a co-ordinated manner supply power to the load at a voltage greater than the input voltage magnitude. The control strategy lies in the manipulation of the duty cycle of the switch which causes the voltage change.

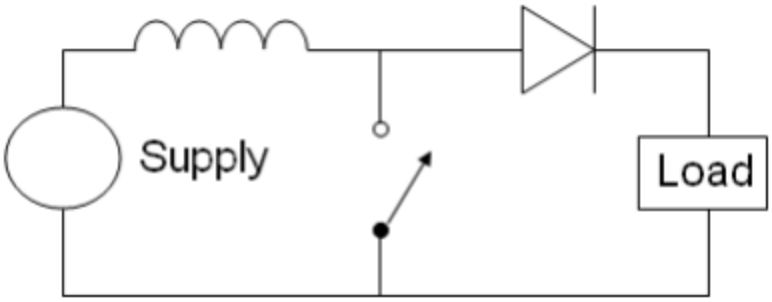

Fig.2 A boost converter

2.2 Modes of Operation

There are two modes of operation of a boost converter. Those are based on the closing and opening of the switch. The first mode is when the switch is closed; this is known as the charging mode of operation. The second mode is when the switch is open; this is known as the discharging mode of operation.

2.2.1 Charging Mode

In this mode of operation; the switch is closed and the inductor is charged by the source through the switch. The charging current is exponential in nature but for simplicity is assumed to be linearly varying. The diode restricts the flow of current from the source to the load and the demand of the load is met by the discharging of the capacitor.

2.2.2 Discharging Mode

In this mode of operation; the switch is open and the diode is forward biased. The inductor now discharges and together with the source charges the capacitor and meets the load demands. The load current variation is very small and in many cases is assumed constant throughout the operation.

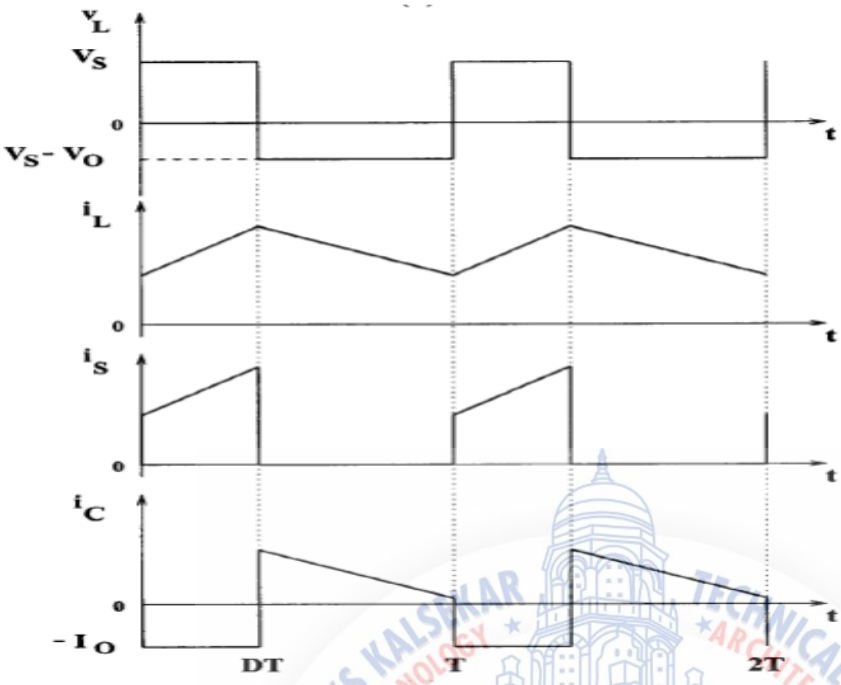

The gain of the boost converter, in the continuous power system, is given by [21];

$$G_{boost} = \frac{V_{o/p}}{V_{i/p}} = \frac{V_{dc}}{V_{PV}} = \frac{1}{1 - D_{boost}}$$

where V_{pv} is the array voltage, V_{dc} is the DC-link average voltage that should be chosen to provide proper modulation index of the inverter and D_{boost} is the chopper duty ratio. The inductance of the boost converter (L_{boost}) is determined by selecting the acceptable current ripple passing through it (ΔI_L) from (2):

$$\Delta I_L = \frac{D_{boost} V_{PV}}{f_{sw(b)} L_{boost}} = \frac{D_{boost}(1 - D_{boost}) V_{dc}}{f_{sw(b)} L_{boost}}$$

where $f_{sw(b)}$ is the switching frequency of the boost converter.

2.3 Decoupling Capacitor at DC-Link

The DC-link capacitor (C_{dc}) is sized according to keep DC-link voltage fluctuations within specified limits ;

$$C_{dc} = \frac{P_g}{\omega V_{dc} \Delta v_{dcp-p}} = \frac{P_g}{2\omega V_{dc} \Delta v_{dc}}$$

where P_g is the average active power injected into the grid, □□is the line angular frequency in rad/sec, Δv_{dcp-p} is the peak to peak DC-link voltage ripple and Δv_{dc} is the amplitude of the DC-link voltage ripple.

2.4 Voltage Source Inverter

Increasing efforts are being made nowadays to use renewable energy sources. Processing the energy obtained from sun, wind or water is coming to the fore. The energy supplied by these sources does not have constant values, but fluctuates according to the surrounding conditions (intensity of sun rays, water flow, etc.). These supplies are therefore supplemented by additional converters. The most used types are inverters or DC/DC converters. The area of high power converters for solar application is already covered by industrial manufacturers. However, the area of low power devices is not fully covered. These converters are mostly built from commercially produced parts that can perform demanded functions, but they are not developed for this type of application and therefore the efficiency of the whole system is low. Low power devices are important in applications where there is no voltage grid present and electric power is required (mountains, desert expeditions, etc.) The simplified block structure of the investigated system is shown in Fig. 1. A DC/DC converter with an MPPT (Maximum Power Point Tracker) is connected to the solar array. A second DC/DC converter is connected to the output of this converter. The second converter raises the voltage acquired from the solar system to the voltage level demanded by the VSI.

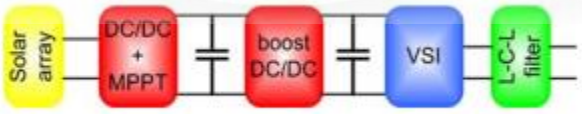

Fig 3 .Block diagram of the system

The VSI is used for converting energy from DC to AC voltage. The detailed scheme of the inverter is shown in the Fig. 3. The power part of the inverter is made of four MOSFETs and the L-C-L filter is connected to the output of the inverter. This filter ensures the sinusoidal shape of the output current.

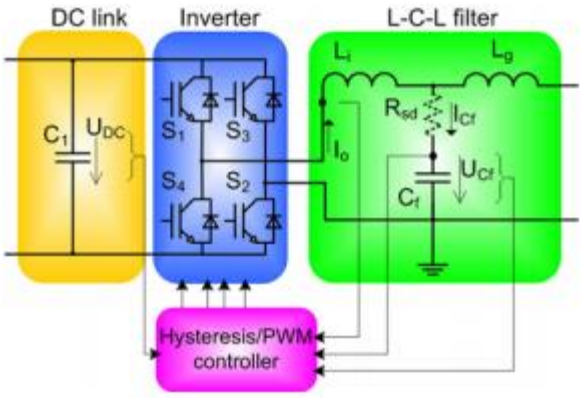

Fig 4.Inverter diagram

The inverter in this application can operate in two different modes. Firstly, it can operate in the so-called "island mode", which means that the converter acts as a voltage source and supplies some devices with sinusoidal voltage of the common network parameters. PWM control is used for this purpose. The second possible operation mode delivers current to the supply network. PWM control is not suitable for this operation mode and the current hysteresis control is therefore used.

2.5 PWM Control

Hysteresis control cannot operate in "island mode", because there is no supply network voltage that can guard the generated voltage. Then the converter is supposed to generate output voltage with a sinusoidal shape, as in the supply network. The PWM control algorithm was therefore used for "island mode". The controller is shown in Fig. 5. The PI controller is used in the voltage control loop. The output of the controller is the duty cycle for the modulator.

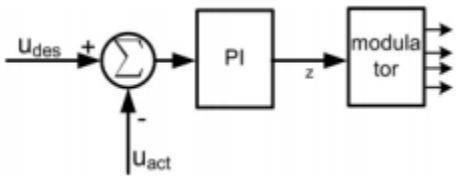

Fig 5 .Island mode control loop

The second stage involves a current controlled full-bridge VSI operating with sinusoidal pulse width modulation (SPWM) and a triangular carrier (15 kHz). The inverter output filter inductor (Lac) is designed to mitigate the harmonics of the injected grid current. For high switching frequency and near unity power factor operation, the output voltage of the inverter is approximately equal to the utility voltage and the modulation index amplitude (ma) is given by

$$m_a = \frac{\hat{V}_g}{V_{dc}}$$

For single-phase inverters, Vdc level is determined such that $m_a \leq 1$ so as to achieve acceptable total harmonic distortion in the grid current (THDI). Hence, Lac is calculated from (5) as follows.

$$\Delta I_g = \frac{V_{dc}}{2 f_{sw(i)} L_{ac}} \frac{1}{2\sqrt{3}} \sqrt{\frac{1}{2} m_a^2 - \frac{8}{3\pi} m_a^3 + \frac{3}{8} m_a^4} \quad (5)$$

where $f_{sw(i)}$ is the switching frequency of the inverter and ΔI_g is the rms ripple component of the grid current and can be calculated from;

$$THDI = \frac{\Delta I_g}{I_{g(1)}} \times 100 \leq THD(required) \quad (6)$$

Where I_g (1) is the root mean square (rms) value of the grid current fundamental component.

CHAPTER 3

MAXIMUM POWER POINT TRACKING

Maximum Power Point Tracking

The efficiency of a solar cell is very low. In order to increase the efficiency, methods are to be undertaken to match the source and load properly. One such method is the Maximum Power Point Tracking (MPPT). This is a technique used to obtain the maximum possible power from a varying source. In photovoltaic systems the I-V curve is non-linear, thereby making it difficult to be used to power a certain load. This is done by utilizing a boost converter whose duty cycle is varied by using a MPPT algorithm. A boost converter is used on the load side and a solar panel is used to power this converter.

3.1 Methods For MPPT

There are many methods used for maximum power point tracking a few are listed below:

- Perturb and Observe method
- Incremental Conductance method
- Parasitic Capacitance method
- Constant Voltage method

3.1.1 Perturb and Observe method

This method is the most common. In this method very less number of sensors are utilized . The operating voltage is sampled and the algorithm changes the operating voltage in the required direction and samples $\frac{dP}{dV}$. If $\frac{dP}{dV}$ is positive, then the algorithm increases the voltage value towards the MPP until $\frac{dP}{dV}$ is negative. This iteration is continued until the algorithm finally 16 reaches the MPP.

3.1.2 Incremental Conductance method

This method uses the PV array's incremental conductance $\frac{dI}{dV}$ to compute the sign of $\frac{dP}{dV}$. When $\frac{dI}{dV}$ is equal and opposite to the value of I/V (where $\frac{dP}{dV}$ = 0) the algorithm knows that the

maximum power point is reached and thus it terminates and returns the corresponding value of operating voltage for MPP. This method tracks rapidly changing irradiation conditions more accurately than P&O method.

$$P=V*I$$

Differentiating w.r.t voltage yields;

$$\frac{dP}{dV} = \frac{d(V*I)}{dV}$$

$$\frac{dP}{dV} = I*\left(\frac{dV}{dV}\right) + V*\left(\frac{dI}{dV}\right)$$

$$\frac{dP}{dV} = I + V*\left(\frac{dI}{dV}\right)$$

When the maximum power point is reached the slope $\frac{dP}{dV} = 0$. Thus the condition would be;

$$\frac{dP}{dV} = 0$$

$$I + V*\left(\frac{dI}{dV}\right) = 0$$

$$\frac{dI}{dV} = -\frac{I}{V}$$

3.1.3 Parasitic Capacitance method

This method is an improved version of the incremental conductance method, with the improvement being that the effect of the PV cell's parasitic union capacitance is included into the voltage calculation .

3.1.4 Constant Voltage method

This method which is a not so widely used method because of the losses during operation is dependent on the relation between the open circuit voltage and the maximum power point voltage. The ratio of these two voltages is generally constant for a solar cell, roughly around 0.76. Thus the open circuit voltage is obtained experimentally and the operating voltage is adjusted to 76% of this value .

Constant Current method Similar to the constant voltage method, this method is dependent on the relation between the open circuit current and the maximum power point current. The ratio of

these two currents is generally constant for a solar cell, roughly around 0.95. Thus the short circuit current is obtained experimentally and the operating current is adjusted to 95% of this value . The methods have certain advantages and certain disadvantages. Choice is to be made regarding which algorithm to be utilized looking at the need of the algorithm and the operating conditions. For example, if the required algorithm is to be simple and not much effort is given on the reduction of the voltage ripple then P&O is suitable. But if the algorithm is to give a definite operating point and the voltage fluctuation near the MPP is to be reduced then the IC method is suitable, but this would make the operation complex and more costly.

3.2 Flow Chart Of MPPT Algorithms

Two of the most widely used methods for maximum power point racking are studied here. The methods are

1. Perturb & Observe Method.
2. Incremental Conductance Method.

The flow charts for the two methods are shown below.

3.2.1 Flow chart for Perturb & Observe:

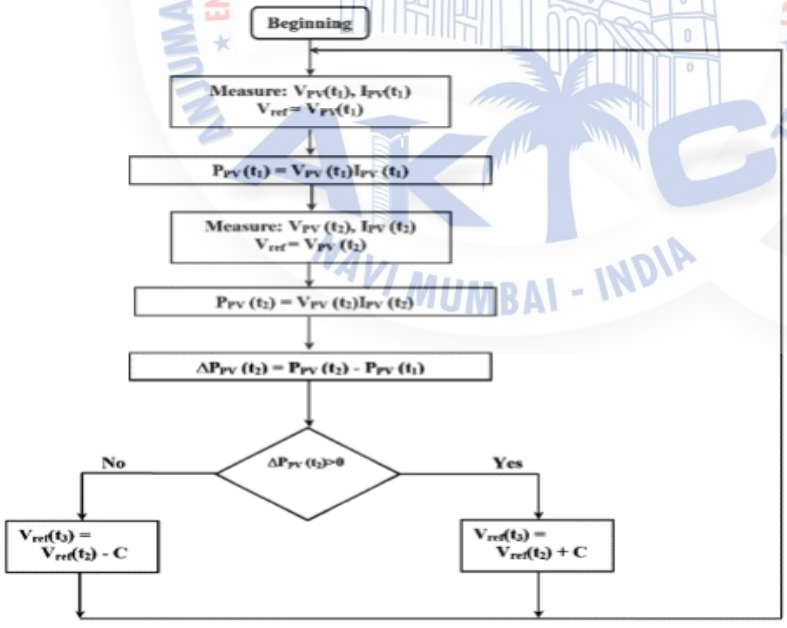

Fig 6 . Flow chart of perturb & observe

3.3.2 Flow chart of incremental conductance method:

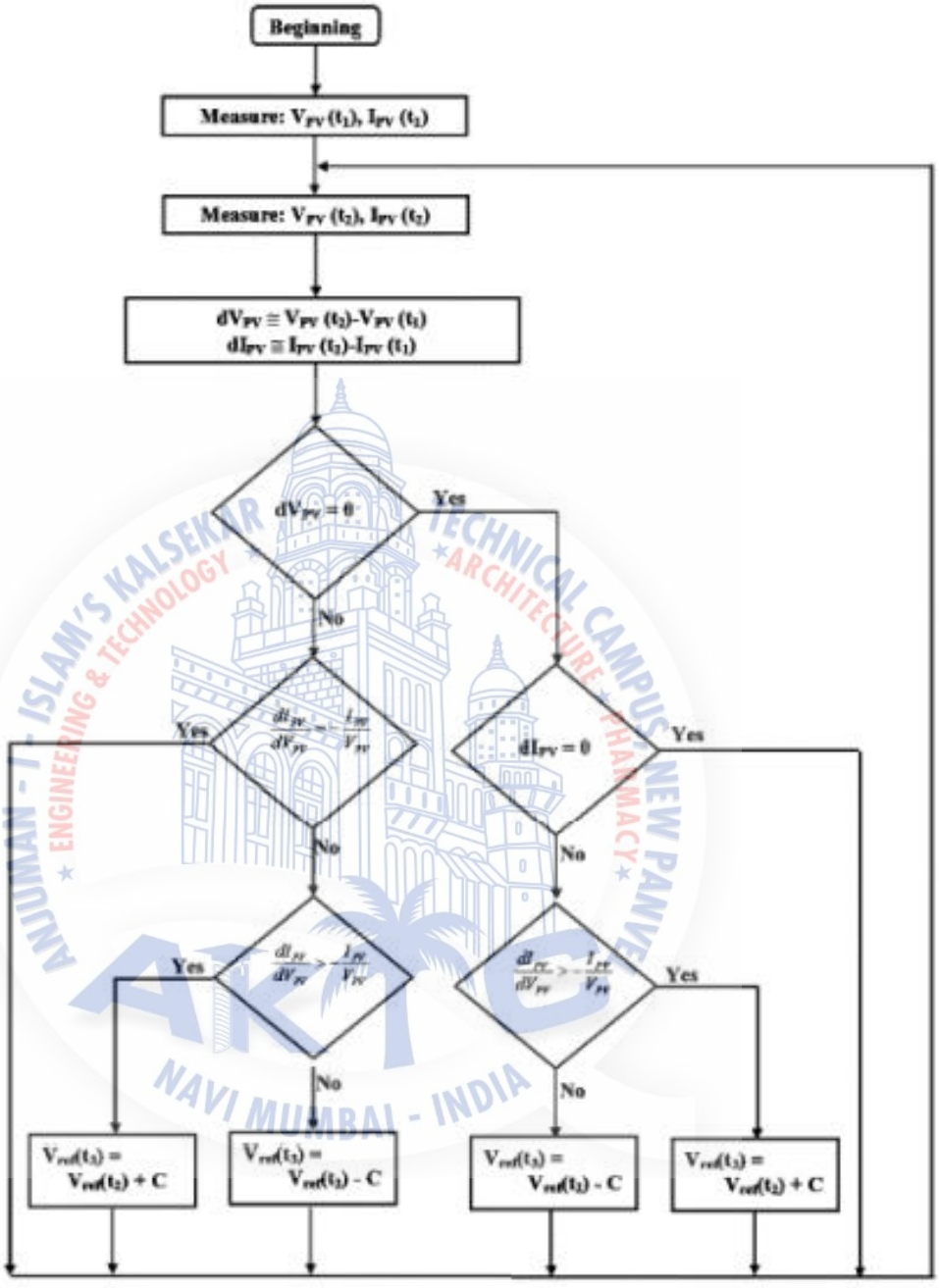

Fig 7 . Flow chart of incremental conductance method

CHAPTER 4

POWER BALANCE AT DC-LINK

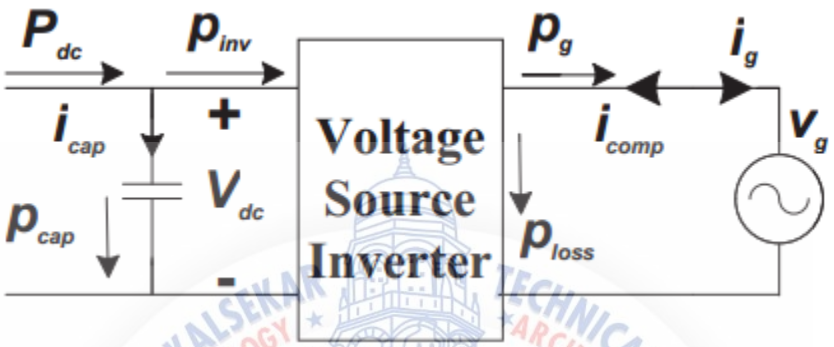

Fig. 8. Power flow at the DC and AC sides of the inverter

Assuming that the AC inductor is small and the AC line current (ig) is sinusoidal and in phase with the AC grid voltage (vg), equation (7) represents the power balance at the inverter DC-link , as shown in Fig. 8.

$$P_{dc} = p_{inv} + p_{cap}$$

where Pdc is the input power to the DC-link, pinv is the instantaneous power supplied to the inverter, pcap is the instantaneous power in the DC capacitor (Cdc)

and

$$p_{cap} = V_{dc} C_{dc} \frac{dv_{dc}}{dt}$$

Hence,

$$P_{dc} = p_{inv} + V_{dc} C_{dc} \frac{dv_{dc}}{dt}$$

where V_{dc}, v_{dc} are the average and the instantaneous values of the DC-link voltage respectively. Power at the inverter DC side (p_{inv}) will then flow through the inverter to the grid. However, inverter losses must be taken into account as shown in (10) otherwise a disturbance into the power balance equation will occur that results in a steady-state error in the DC-link voltage .

$$P_{dc} = p_g + p_{loss} + V_{dc}C_{dc}\frac{dv_{dc}}{dt}$$

where, p_g is the instantaneous active power injected to grid and p_{loss} is the instantaneous inverter power loss. To guarantee the previous power flow, the DC-link voltage is kept constant. Consequently, the term $\frac{dv_{dc}}{dt}$ tends to zero over one cycle and the DC-link power balance is satisfied. Hence, a control strategy is mandatory to achieve DC-link voltage regulation and grid interface.

CHAPTER 5

PV-GRID INTERFACE CONTROL TECHNIQUES

PV-utility interface can be achieved, for the considered system, using conventional control technique . However, a DC-link voltage sensorless technique is proposed to realize this interface. The control schemes of both techniques are analyzed, and then their performance is compared to validate the feasibility of the proposed one.

5.1 Conventional Control Technique

The conventional control technique is shown in Fig. 9. Switching of the boost chopper is directly controlled using variable step incremental conductance MPPT algorithm . On the other hand, DC-link voltage regulation and interface with utility are conventionally achieved by two control loops inhibited in the VSI; the outer DC-link voltage and the inner grid current control loops.

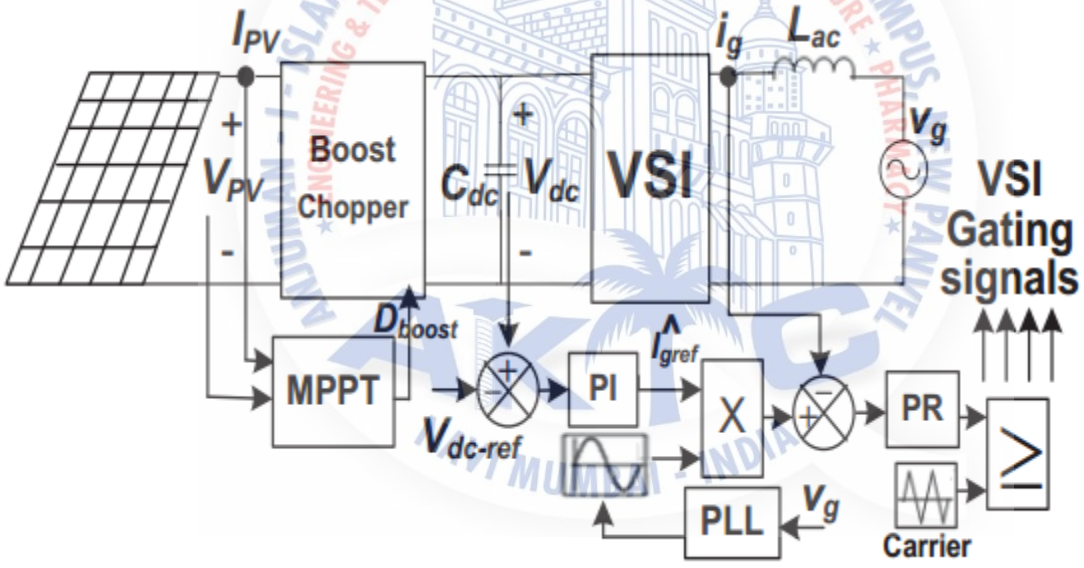

Fig. 9. Conventional control technique scheme

5.1.1 Inner Grid Current Control Loop:

The inverter is required to inject a sinusoidal grid current with low THD and in phase with the grid voltage. Thus, the output of the DC link voltage controller, which represents the reference grid current amplitude, is multiplied by a sinusoidal template obtained using a phase-locked loop (PLL) synchronized with the utility voltage. The current controller attempts to match the grid

current with this reference sinusoidal current. The most common types of current controllers are: the proportional integral (PI) with feed forward controller and the proportional resonant (PR) controller. However, PR controllers have the ability to remove both the current's magnitude and phase steady-state errors without the need of voltage feed forward unlike the conventional PI controllers.

Thus a PR controller is considered with a transfer function given by;

$$G_{PR}(s) = K_P + K_I \frac{s}{s^2 + \omega^2}$$

where Kp is the proportional gain, Ki is the resonant part gain and w is the resonant frequency of the controller which is the grid voltage angular frequency.

5.1.2 Outer DC-link Voltage Control Loop:

This loop is responsible for DC-link voltage regulation by adjusting the amplitude of the sinusoidal reference grid current ($\widehat{I_{gref}}$). This current amplitude represents the active component of the reference grid current which indicates the instantaneous amount of power available at the DC side of the inverter (pinv) . By accurate adjusting to this current amplitude and using a fast grid current controller of a bandwidth of a few kHz, power at the inverter side is transferred to the grid. Thus, power balance at the DC-link is achieved which makes Vdc stabilizes at the required level.

However, in order to compensate for system losses (i.e. inverter losses and the energy required by Cdc to keep Vdc at a certain level), a decrease in the power available at the inverter side occurs which in turn decreases $\widehat{I_{gref}}$. The latter imposes losses on the utility grid.

The DC-link voltage controller can be implemented as a simple proportional controller or proportional integral (PI) one to minimize the DC-link voltage steady-state error . The latter is applied and represented by the transfer function given in (14) where Kp and KI are the applied controller's proportional and integral gains respectively,

$$G_{PI}(S) = K_P + \frac{K_I}{s}$$

However, the DC-link voltage controller must be precisely tuned to limit the oscillations reflected in the grid current reference. Otherwise, grid current THD can exceed the limit and a larger DC capacitor may be required, to overcome these oscillations, which in turn reduces the inverter life-time. Hence, this loop controller is designed for a low cross-over frequency (10-20 Hz) in order to attenuate the magnitude of the DC-link voltage ripple with double line frequency (100 Hz) .

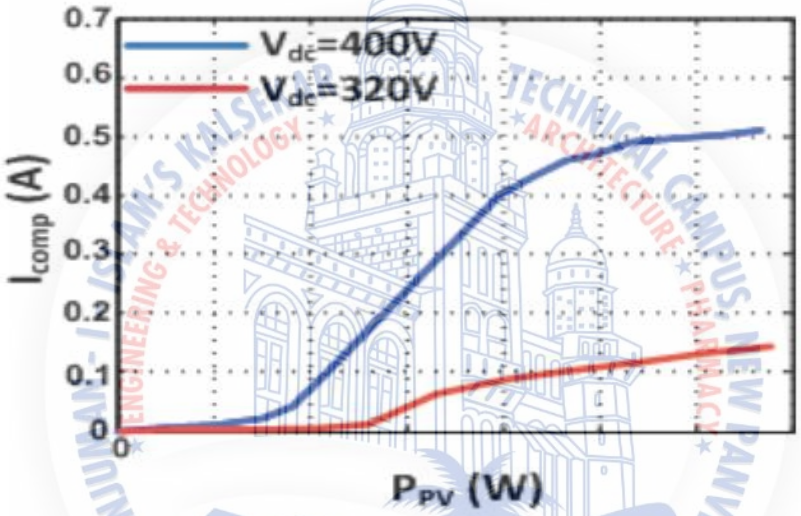

Fig. 10. Mapping between P_{PV} and I_{com}

At certain V_{dc}, as P_{PV} increases system losses increase which requires the increase of I_{comp} to compensate for these losses. Hence, for constant V_{dc}, I_{comp} depends on P_{PV} and changes proportionally with it however in a non-linear form. Moreover, as V_{dc} increases, for constant P_{PV}, energy acquired by the DC-link capacitor increases which results in an increase in I_{comp} to compensate for this energy. Figure 10 shows the non-linear relation between P_{PV} and I_{comp} for two different V_{dc} values. It can be noticed that at V_{dc}=320V (i.e. $m_a \approx 1$), I_{comp} has lower value which in turn decreases utility losses.

Hence, mapping between P_{PV} and I_{comp}, at a predetermined V_{dc} level, is system-dependent and mandatory in order to achieve the proposed DC-link voltage sensor-less scheme. The P_{PV}-I_{comp}

mapping can be implemented using a simple look-up table. However, for more precise mapping and better system performance, a simple feed-forward back-propagation neural network (NN) is created and utilized in the proposed technique . It consists of an input layer, one hidden layer and an output layer as shown in Fig. 11. The input represents the PV power while the output layer gives the compensating current which corresponds to the input PV power and is required to stabilize V_{dc} at a predetermined level. The applied hidden layer features 10 sigmoid neurons. Successful fitting between P_{PV} and I_{comp} depends on the hidden layer and how well the NN is trained to optimize the weights of links between nodes. The utilized NN is off-line trained where the number of the applied training epochs is ten to give almost zero mean square error for the studied case.

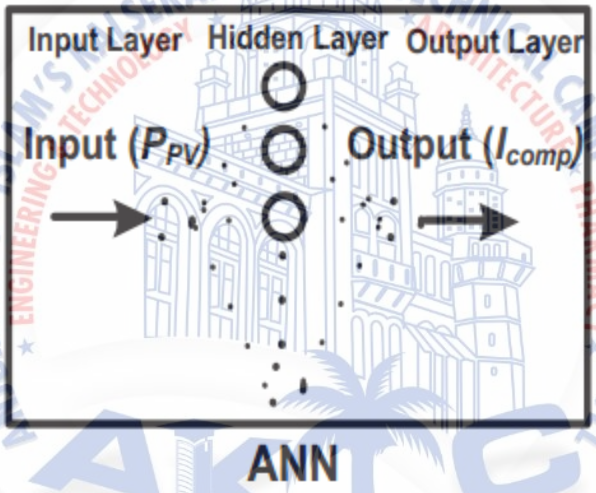

Fig 11. Appllied neural network configurtion

CHAPTER 6
SIMULATION RESULTS

The transient and steady-state performance of the conventional scheme is compared to that of the proposed, under two step changes in irradiance; from 1000 W/m2 to 600 W/m2 at 0.6 sec then from 600 W/m2 to 800 W/m2 at 0.9 sec. The DC-link voltage is adjusted at 320V to decrease utility power losses as described in the previous subsection.

As shown in Fig. 11, both techniques succeed in extracting PV maximum power for different irradiance levels. Fig. 8 shows that the DC-link voltage, for both schemes, stabilizes at 320V. Finally, Fig. 9 shows the grid current acquired by both techniques during irradiance changes. Simulation results are analyzed and performance parameters are given in Table I. At system start-up (Table I), V_{dc} overshoot in the conventional technique is larger than that of the proposed one by about 80 V, thus C_{dc} of the former must handle this voltage increase. On the other hand, V_{dc} adjustment takes much more time, in the proposed scheme, which increases transient power losses. However, once the required V_{dc} level is reached, the proposed scheme shows better transient response for sudden irradiance changes, due to the elimination of outer loop controller. This is shown as follows;

During the first irradiance step change at t=6sec, radiation decreases, thus P_{pv} will decrease causing a transient decrease in V_{dc} till it is regulated to 320V. Analyzing Fig. 8.b, 9.b and Table I, the conventional control scheme shows slower response by about 0.3 sec. Furthermore, it experiences V_{dc} which transiently decreases to 300V i.e. $m_a > 1$. Thus, the grid current THD goes transiently beyond acceptable limits (=31.42 %) according to IEEE Std. 519 [26]. On the other hand, the proposed technique shows faster response and transient V_{dc} decrease to 310 V i.e. $m_a \approx 1$. Hence, its grid current THD iswithin limits (= 6.3%) during its transient period.

During the second irradiance step change at t= 9 sec, radiation increases, thus P_{PV} increases causing transient increase in V_{dc} .Considering Table I, the conventional scheme exhibits longer settling time and transient V_{dc} increase to 360V causing transient increase in

utility power loss by almost 25% of its steady-state value (80W). However, the proposed scheme shows almost non significant V_{dc} increase during its transient period.

Finally, considering the steady-state results shown in Table I, both schemes gave close results which proves the validity and feasibility of the proposed technique.

TABLE I

TRANSIENT AND STEADY-STATE PERFORMANCE PARAMETERS

Irradiance (W/m^2)	Con. Tech	Transient for V_{dc}		Steady-state			
		Over/ Under Shoot	$t_{sett.}$ (sec)	Δv *p-p*	*Power losses*	*THD*	*Phase shift*
Start-1000W/m^2	Conv.	+ 68.75%	0.4	50V	92 W	3%	1°
	Prop.	+ 43.75%	4	50V	98 W	2%	0°
From 1000 to 600W/m^2	Conv.	– 6.25%	0.4	30V	74.5W	3.8%	0.8°
	Prop.	– 3.13%	0.1	30V	74.8W	3%	0.1°
From 600 to 800W/m^2	Conv.	+ 12.5 %	0.2	40V	80W	3.2%	1°
	Prop.	+1.5%	0.07	40V	80.5W	2.2%	0°

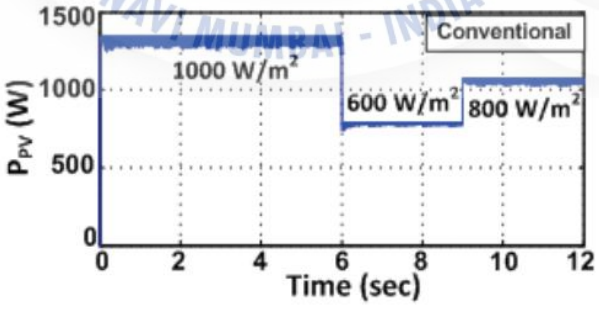

Fig. 12. Maximum power extracted from PV string using conventional techniques at three different irradiance levels

CHAPTER 7
MATLAB

7.1 Introduction:

Matlab is a high-performance language for technical computing. The name mat lab stands for matrix laboratory. It integrates computation, visualization, and programming in an easy-to-use environment where problems and solutions are expressed in familiar mathematical notation. Typical uses include Math and computation Algorithm development Data acquisition Modeling, simulation, and prototyping Data analysis, exploration, and visualization Scientific and engineering graphics Application development, including graphical user interface building.

7.2 Strengths:

- MATLAB is relatively easy to learn.
- MATLAB code is optimized to be relatively quick when performing matrix operations.
- MATLAB may behave like a calculator or as a programming language.
- MATLAB is interpreted, errors are easier to fix.
- Although primarily procedural, MATLAB does have some object-oriented elements.

7.3 Other features:

- 2-D and 3-D graphics functions for visualizing data
- Tools for building custom graphical user interfaces
- Functions for integrating MATLAB based algorithms with external applications and languages, such as C, C++, FORTRAN, Java, COM, and Microsoft Excel.

7.4 Components:

- Workspace
- Current Directory
- Command History
- Command Window

7.5 Toolboxes :

- Simulink
- Fuzzy
- Genetic algorithm
- Neural network
- Wavelet

7.6 Applications:

Some of the mat lab applications listed are:

- Orthogonal frequency division multiplexing
- Genetic algorithm data mining
- Speech recognition using VQ method
- Channel Estimation and Detection in DS-CDMA
- Analysis of iterative channel estimation and multi-user detection in multi path DS-CDMA channels

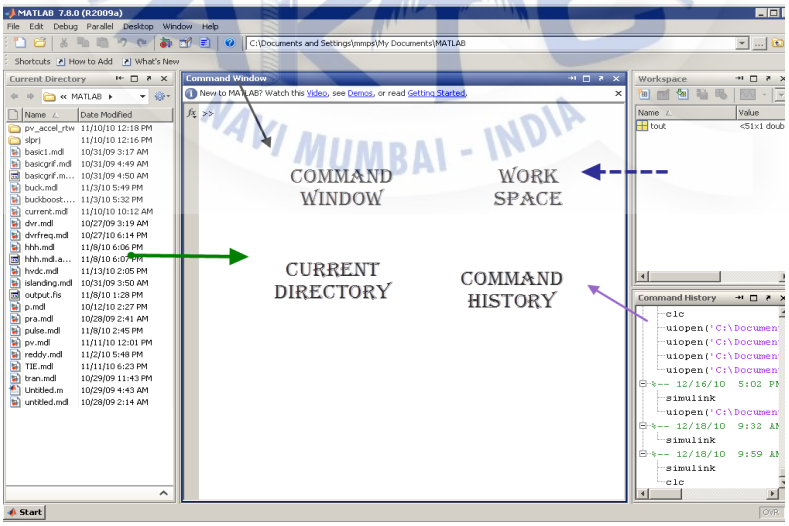

Block diagram of Mat lab components

CHAPTER 8

SIMULINK

8.1 Introduction:

Simulink is a software add-on to mat lab which is a mathematical tool developed by The Math works,(http://www.mathworks.com) a company based in Natick. Mat lab is powered by extensive numerical analysis capability. Simulink is a tool used to visually program a dynamic system (those governed by Differential equations) and look at results. Any logic circuit, or control system for a dynamic system can be built by using standard building blocks available in Simulink Libraries. Various toolboxes for different techniques, such as Fuzzy Logic, Neural Networks, DSP, Statistics etc. are available with Simulink, which enhance the processing power of the tool. The main advantage is the availability of templates / building blocks, which avoid the necessity of typing code for small mathematical processes.

8.2 Concept of signal and logic flow:

In Simulink, data/information from various blocks are sent to another block by lines connecting the relevant blocks. Signals can be generated and fed into blocks dynamic / static).Data can be fed into functions. Data can then be dumped into sinks, which could be scopes, displays or could be saved to a file. Data can be connected from one block to another, can be branched, multiplexed etc. In simulation, data is processed and transferred only at discrete times, since all computers are discrete systems. Thus, a simulation time step (otherwise called an integration time step) is essential, and the selection of that step is determined by the fastest dynamics in the simulated system.

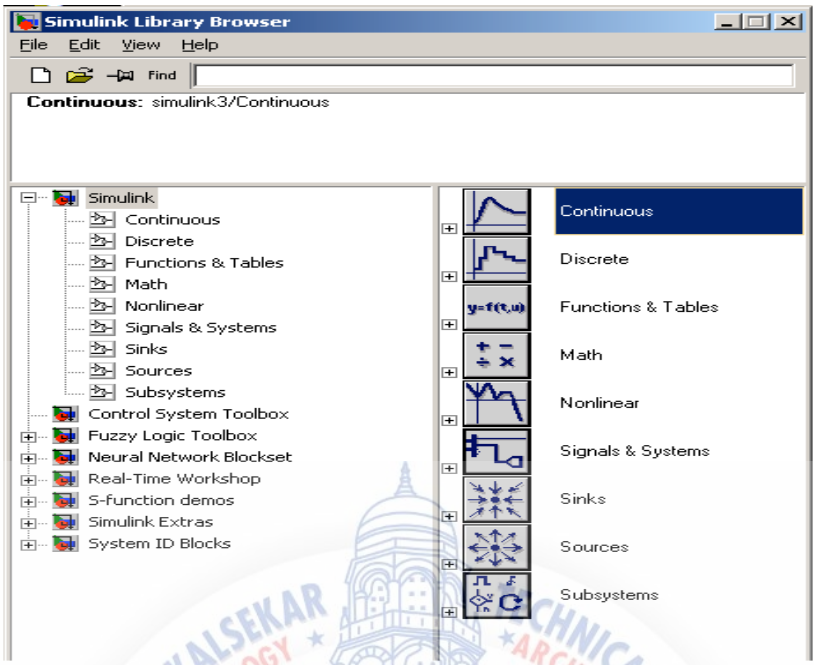

Fig 13. Simulink library browser

8.2.1 Sources and sinks:

The sources library contains the sources of data/signals that one would use in a dynamic system simulation. One may want to use a constant input, a sinusoidal wave, a step, a repeating sequence such as a pulse train, a ramp etc. One may want to test disturbance effects, and can use the random signal generator to simulate noise. The clock may be used to create a time index for plotting purposes. The ground could be used to connect to any unused port, to avoid warning messages indicating unconnected ports.

The sinks are blocks where signals are terminated or ultimately used. In most cases, we would want to store the resulting data in a file, or a matrix of variables. The data could be displayed or even stored to a file. The stop block could be used to stop the simulation if the input to that block (the signal being sunk) is non-zero. Figure 3 shows the available blocks in the sources and sinks libraries. Unused signals must be terminated, to prevent warnings about unconnected signals.

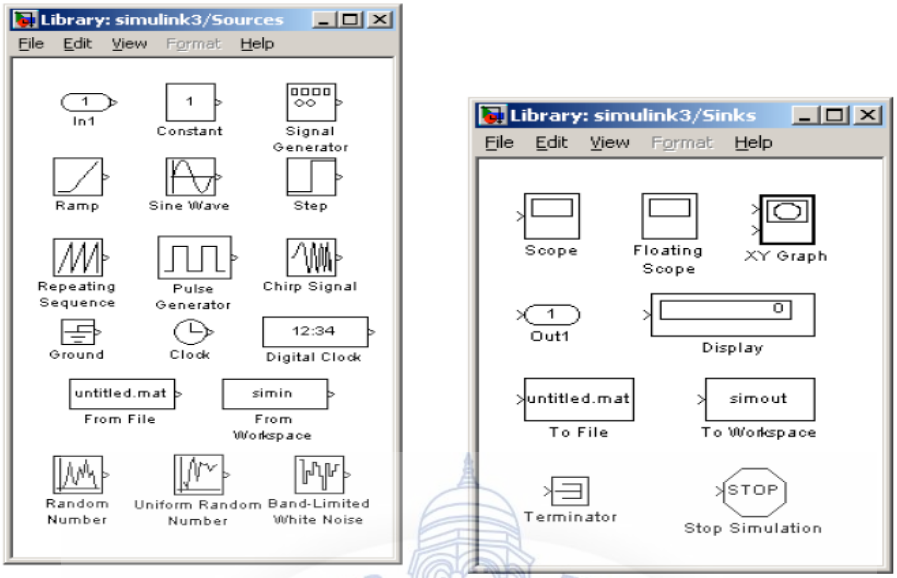

Fig 15. Sources and sinks

8.3 Continuous and discrete systems:

All dynamic systems can be analyzed as continuous or discrete time systems. Simulink allows you to represent these systems using transfer functions, integration blocks, delay blocks etc.

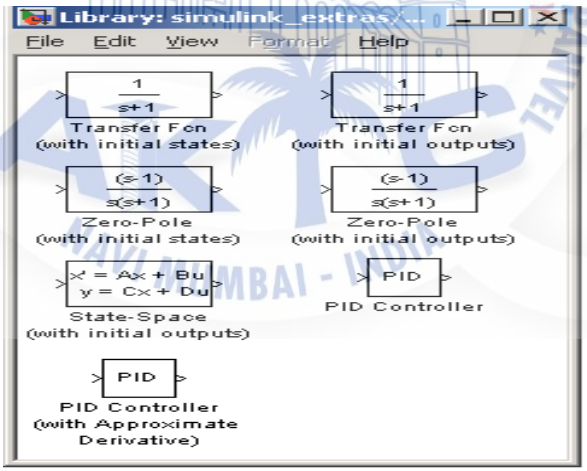

fig 16 continous and descrete systems

8.4 Non-linear operators:

A main advantage of using tools such as Simulink is the ability to simulate non-linear systems and arrive at results without having to solve analytically. It is very difficult to arrive at an analytical solution for a system having non-linearities such as saturation, signup function,

limited slew rates etc. In Simulation, since systems are analyzed using iterations, non-linearities are not a hindrance. One such could be a saturation block, to indicate a physical limitation on a parameter, such as a voltage signal to a motor etc. Manual switches are useful when trying simulations with different cases. Switches are the logical equivalent of if-then statements in programming.

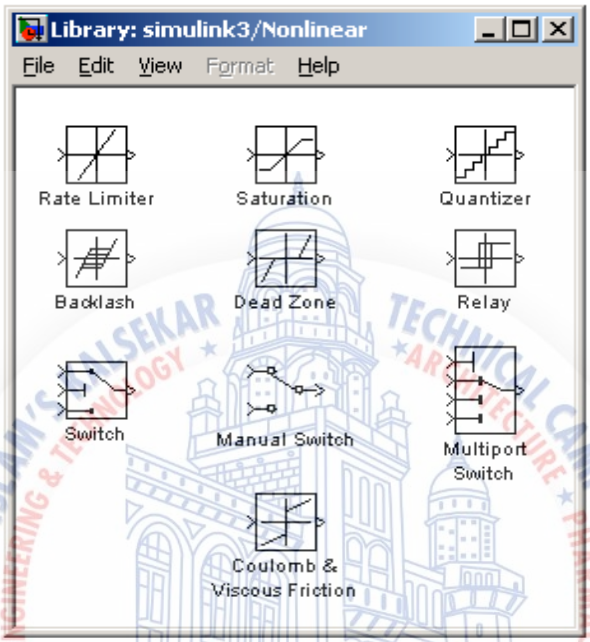

Fig 17. simulink blocks

8.5 Signals & data transfer:

In complicated block diagrams, there may arise the need to transfer data from one portion to another portion of the block. They may be in different subsystems. That signal could be dumped into a GOTO block, which is used to send signals from one subsystem to another.

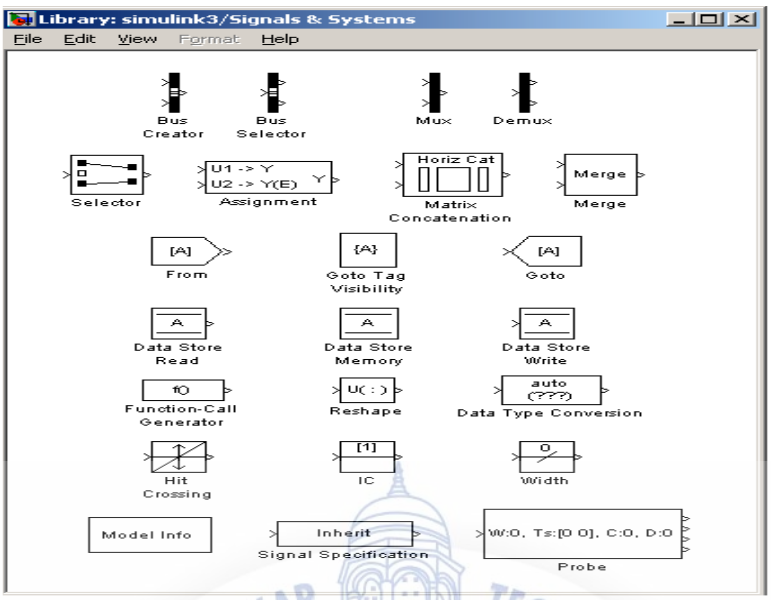

Fig 19. signals and systems

Multiplexing helps us remove clutter due to excessive connectors, and makes matrix (column/row) visualization easier.

8.6 Setting simulation parameters:

Running a simulation in the computer always requires a numerical technique to solve a differential equation. The system can be simulated as a continuous system or a discrete system based on the blocks inside. The simulation start and stop time can be specified. In case of variable step size, the smallest and largest step size can be specified. A Fixed step size is recommended and it allows for indexing time to a precise number of points, thus controlling the size of the data vector. Simulation step size must be decided based on the dynamics of the system. A thermal process may warrant a step size of a few seconds, but a DC motor in the system may be quite fast and may require a step size of a few milliseconds.

CHAPTER 9

CONCLUSION

This paper proposes a novel DC-link voltage control technique, for single-phase two-stage PV-grid connected systems, which eliminates the DC-link voltage control loop. Alternatively, a new adjustment method of reference grid current is presented to transfer the PV power to the utility. Thus, energy balance is achieved at the DC-link and DC voltage stabilizes at a predetermined level. Consequently, control scheme complexity is minimized and system stability is enhanced. Moreover, high DC-link voltage sensor elimination reduces the system size and cost. Simulation results are analyzed to evaluate proposed technique performance and compare it with that of the proposed one. Although the novel technique is slower to stabilize the DC-link voltage at start-up, once the required DC-link voltage is reached, the proposed technique shows better transient response during sudden irradiance changes. At steady-state, both techniques give close results, which validates the proposed technique effectiveness.

REFERENCES

[1] M. Liserre, T. Sauter, and J. Y. Hung, "Future energy systems: Integrating renewable energy sources into the smart power grid through industrial electronics", IEEE Industrial Electronics Magazine, vol. 4, no.1, pp.18-37, March 2010.

[2] S. V. Araújo, P. Zacharias, and R. Mallwitz, "Highly efficient singlephase transformerless inverters for grid-connected photovoltaic systems ", IEEE Trans. Industrial Electronics, vol. 57, no. 9, pp. 3118-3128, Sep. 2010

[3] S. B. Kjaer, J. K. Pedersen, and F. Blaabjerg," A review of single-phase grid-connected inverters for photovoltaic modules", IEEE Trans. Industry Applications, vol. 41, no. 5, pp.1292-1306, Sep/Oct 2005

[4] J. Myrzik and M. Calais, "String and module integrated inverters for single-phase grid connected photovoltaic systems - a review," in Proc. IEEE Power Tech Conf., vol. 2, June 2003.

[5] S. Chowdhury, S.P. Chowdhury and P. Crossley, Microgrids and Active Distribution Networks, IET Renewable Energy Series 6, Institution of Engineering and Technology, London, 2009

[6] F. Blaabjerg, R. Teodorescu, M. Liserre, and A. V. Timbus, " Overview of control and grid synchronization for distributed power generation systems", IEEE Trans. Industrial Electronics, vol. 53, no. 5, pp. 1398- 1409, October 2006.

[7] M. A. Eltawil, and Z. Zhao, " Grid-connected photovoltaic power systems: Technical and potential problems—A review", ELSEVIER Trans. Renewable and Sustainable Energy Reviews, vol. 14, no. 1, pp. 112–129, January 2010.

[8] S. Jain and V. Agarwal, "A single-stage grid connected inverter topology for solar PV systems with maximum power point tracking," IEEE Trans. Power Electronics, vol. 22, pp. 1928–1940, Sept. 2007.

[9] S. Jain, and V. Agarwal, "Comparison of the performance of maximum power point tracking schemes applied to single-stage grid-connected photovoltaic systems," IET Electric Power Applications, vol. 1, no. 5, pp. 753-762, Sept. 2007.